AEDC-TR-72-132

cy2

COLLISIONAL DE-EXCITATION CROSS-SECTION MEASUREMENT OF ELECTRONIC STATES OF ATOMIC AND MOLECULAR HYDROGEN BY COLLISION WITH MOLECULAR HYDROGEN

J. W. L. Lewis and W. D. Williams

ARO, Inc.

October 1972

VON KÁRMÁN GAS DYNAMICS FACILITY
ARNOLD ENGINEERING DEVELOPMENT CENTER
AIR FORCE SYSTEMS COMMAND
ARNOLD AIR FORCE STATION, TENNESSEE

NOTICES

When U. S. Government drawings specifications, or other data are used for any purpose other than a definitely related Government procurement operation, the Government thereby incurs no responsibility nor any obligation whatsoever, and the fact that the Government may have formulated, furnished, or in any way supplied the said drawings, specifications, or other data, is not to be regarded by implication or otherwise, or in any manner licensing the holder or any other person or corporation, or conveying any rights or permission to manufacture, use, or sell any patented invention that may in any way be related thereto.

Qualified users may obtain copies of this report from the Defense Documentation Center.

References to named commercial products in this report are not to be considered in any sense as an endorsement of the product by the United States Air Force or the Government.

COLLISIONAL DE-EXCITATION CROSS-SECTION MEASUREMENT OF ELECTRONIC STATES OF ATOMIC AND MOLECULAR HYDROGEN BY COLLISION WITH MOLECULAR HYDROGEN

J. W. L. Lewis and W. D. Williams
ARO, Inc.

FOREWORD

The work reported herein was sponsored by the Arnold Engineering Development Center (AEDC), Air Force Systems Command (AFSC), Arnold Air Force Station, Tennessee under Program Element 65802F.

The results of the research presented here were obtained by ARO, Inc. (a subsidiary of Sverdrup & Parcel and Associates, Inc.), contract operator of AEDC under F40600-72-C-0003. The work was conducted under ARO Project Nos. VW5216 and VW5220 from July 1, 1971 to March 1, 1972. The manuscript was submitted for publication on June, 14, 1972.

The authors express their appreciation to A. D. Killian for his aid in operation and maintenance of the apparatus.

This technical report has been reviewed and is approved.

MAURICE A. CLERMONT
Captain, CF
Research and Development Division
Directorate of Technology

ROBERT O. DIETZ
Acting Director
Directorate of Technology

ABSTRACT

The H_α, H_β, and H_γ lines of the Balmer series of atomic hydrogen and the $G^1\Sigma_g^+ \rightarrow B^1\Sigma_u^+$ molecular hydrogen system were produced by 40-kev electron beam excitation of molecular hydrogen at room temperature. The collisional de-excitation cross section of the above-mentioned excited electronic states in collision with $H_2 X^1\Sigma_g^+$ was measured.

CONTENTS

APPENDIXES

I. ILLUSTRATIONS

Figure

NOMENCLATURE

A_i	Einstein spontaneous emission coefficient, sec^{-1}
A_{ij}/A_i	Branching Factor
a_o	First Bohr radius
C	Constant
d_i	Collision diameter of specie i
d_{ij}	Effective collision diameter of species i and j
e	Electronic charge and electron
H_α	α line of Balmer series
H_β	β line of Balmer series
H_γ	γ line of Balmer series
h	Planck's constant
$h\nu$	Photon of energy $h\nu$
I	Electron beam current
k_i	Quenching rate constant of specie i, cc/sec/molecule
L	Electron beam length observed by optics, cm
M	Molecular weight, gm/mole
M_{cl}	Mach number for centerline of flow tube
N	Gas number density, molecules/cc
Pr	Prandtl number
R	Universal gas constant, cgs

Re	Reynolds number
r	Atomic electron radius
$S(\omega)$	Photon emission rate, sec^{-1}
$s(\lambda)$	Wavelength dependent quantum yield
T	Temperature, °K
x/D	Ratio of axial distance to tube diameter
γ	Ratio of constant pressure to constant volume specific heat
λ	Wavelength, Å
σ_{gi}	Electron-molecule cross section for g→i excitation, cm^2
σ_i^2	Variance of measured quantity for determination number i
$\sigma^2(ij)$	Inelastic partial cross section for the i to j transition, cm^2
σ_M^2	Variance of the set of all data
$\sigma_{el}^2(i)$	Elastic cross section of specie i, cm^2
$\sigma_{in}^2(i)$	Inelastic cross section of specie i, cm^2
τ_i	Lifetime of state i, sec
ω	Detector solid angle subtended at the excitation volume, sr

SECTION I
INTRODUCTION

1.1 BACKGROUND

The use of the electron beam fluorescence technique for flow-field diagnostics is an established method for experimentally determining local values of gas density and temperature (Refs. 1, 2, and 3). However, the majority of previous applications has been to flow fields comprised of either common gases, such as N_2, O_2, and air, or noble gases, such as He and Ar, and their mixtures. Diagnostics of other flow fields of current interest such as rocket engine exhausts and flowing gas laser systems presents additional difficulties in that the number of flow-field constituents can be quite large and, also, the appropriate electron beam excitation cross sections and the collisional de-excitation, or quenching , cross sections are in many cases unknown. This absence of required data is exemplified by gaseous molecular hydrogen, H_2, which is a constituent found in the above-mentioned types of flow fields. Although previous investigations (Refs. 4 and 5) of electron beam collisions with H_2 have been made, the purpose of the measurements was the elucidation of the various excitation processes of the collision and, as a result, the highest beam energy employed has been 6 kev (Ref. 5), far less than the typical value of 40 kev used for flow-field diagnostics. As the results of Vroom and deHeer (Ref. 5) demonstrate, the excitation of atomic hydrogen, H, radiation systems, the predominant radiating species of the gas, is only partially optically allowed, and, consequently, extrapolation using a Fano diagram of excitation cross sections acquired at 6 kev to an electron beam energy of 40 kev should be avoided. Additionally, no excitation cross-section data of excited molecular H_2 states exist. As the gas density increases, the probability of collision between the electronically excited atom or molecule and the ground state species become larger, and effects of collisional quenching on the radiation intensity of the excited species must be taken into account and, at present, quenching cross-section data of atomic and molecular hydrogen are rare. For these reasons a study of excitation and de-excitation cross sections of electronic states of H and H_2 was initiated, and the results of the measurements of collisional de-excitation of the H(n = 5, 4, and 3) and $H_2G^1\Sigma_g^+$ states by $H_2X^1\Sigma_g^+$ are presented in this report.

1.2 ELECTRON BEAM EXCITATION OF HYDROGEN

The various excitation processes of H_2 by collision with a high energy electron beam include the following

$$e + H_2 \longrightarrow H + H^{**} + e \qquad (1)$$
$$\hookrightarrow H^{*} + h\nu$$

$$e + H_2 \longrightarrow H^{+} + H^{**} + 2e \qquad (2)$$
$$\hookrightarrow H^{*} + h\nu$$

$$e + H_2 \longrightarrow H_2^{**} + e \qquad (3)$$
$$\hookrightarrow H_2^{*} + h\nu$$

Equation (1) shows the dissociative excitation mechanism which results in two neutral H atoms, one of which is in an excited state represented by H^{**} which then decays radiatively to a lower state H^{*} by the emission of a photon $h\nu$. Equation (2) represents dissociative-ionization, resulting in atomic radiation, and Eq. (3) shows the excitation process for excited electronic states of H_2. No stable H_2^{+} states are known to exist (Ref. 6). Included among the states excited by the processes of (1) and (2) are the H(n = 3, 4, 5) atomic states, and Fig. 1 shows a simplified energy level diagram of H. The radiative transitions available to the H(n = 3, 4, 5) states are indicated in Fig. 1 (Appendix I).

As shown in Fig. 1, the following transitions, the Balmer series of H, are available for observation (Ref. 5) in the visible spectral region:

$$H(n = 5) \longrightarrow H(n = 2) + h\nu \ (4340.5\ \text{Å}) \qquad (4)$$

$$H(n = 4) \longrightarrow H(n = 2) + h\nu \ (4861.3\ \text{Å}) \qquad (5)$$

and

$$H(n = 3) \longrightarrow H(n = 2) + h\nu \ (6562.8\ \text{Å}) \qquad (6)$$

where Eqs. (4) through (6) are known as the H_γ, H_β, and H_α systems, respectively. These particular transitions are the result of either dissociative excitation or ionization processes and, therefore, should be relatively insensitive to the vibrational or rotational temperatures of the $H_2 X^1\Sigma_g^+$ molecules. Additionally, resonance absorption effects are absent for the Balmer series, and, therefore, the Balmer series of atomic transitions is a reasonable choice for use for flow-field diagnostics of local H_2 density.

Several emission lines observed at approximately 4634 Å are tentatively identified as various P and R branch transitions of the (0, 0) band of the H_2 $G^1\Sigma_g^+(3d\sigma) \longrightarrow B^1\Sigma_u^+(2p\sigma)$ electronic transition. Using the potential constants given by Herzberg (Ref. 7) for the G and B states of H_2, wavelengths for the possibly observed R and P branch (0, 0) band

transitions were calculated and are listed in Table I (Appendix II). From Table I it is seen that within ±5 Å of 4634 Å are found the R(1) to R(5) and P(0) rotation-vibration transitions, and the open band structure of the H_2 molecule is quite evident. It is of interest to note that the electron-molecule excitation process, as represented by Eq. (3) is first-order forbidden in that the excitation

$$e + H_2 X^1\Sigma_g^+ \longrightarrow e + H_2\ G^1\Sigma_g^+ \tag{7}$$

does not obey the optical dipole selection rule g⟶u, g⟶g. Similar electron beam-excited emission of H_2 at 4634 Å was observed by Kruithof and Ornstein (Ref. 8) using 30-ev electrons, but unfortunately no excitation cross-section data exist. Figure 2 shows several of the H_2 electron states and diagrams the G to B transition.

For sufficiently low gas density at which collisional quenching effects are negligible, the radiated photon intensity S detected by an optical system of solid angle ω(sr) and quantum yield s(λ) is given by

$$S = \left(\frac{\omega}{4\pi}\right) \cdot \left(\frac{I}{e}\right) \cdot N \cdot L : s(\lambda) \cdot \frac{A_{ij}}{A_i} \cdot \sigma_{gi} \tag{8}$$

where σ_{gi} is excitation cross section for the ground-state level g⟶i transition, L is the observed length of the electron beam of current I, N is the ground-state number density, and cascading has been neglected. For molecular radiative transitions the Einstein coefficient is replaced by the electronic rotation-vibration transition line strength. On the basis of the results of Ref. 5, polarization effects are ignored, and the viewing direction is assumed to be perpendicular to the beam. Equation (8) shows the linear dependence of S on the ground-state molecular number density N.

In the event of radiative cascading from upper excited states into level i, it is easily shown that Eq. (8) remains as written if the cross section σ_{gi} is replaced by

$$\sigma_{gi} + \sum_t (A_{ti}/A_t) \cdot \sigma_{gt}$$

and the summation is over all states t for which the energy eigenvalue E_t exceeds that of state i, E_i.

1.3 COLLISIONAL DE-EXCITATION OF THE RADIATING STATE

As the molecular hydrogen density is increased one must allow for collisional de-excitation of the H(n = 3, 4, 5) and the $H_2\ G^1\Sigma_g^+$ states,

assuming binary collisions to be the appropriate collision mechanism. Collision of two excited species is negligible for the gas density regime of interest. The quenching process of the atomic and molecular hydrogen states is shown in Eqs. (9a) and (9b) and is nonspecific in the sense that the final states n_x, n_y, and X, Y radiating and quenching are unknown:

$$H(n = 3,\ 4,\ 5) + H_2\,{}^1\Sigma_g^+ \xrightarrow{k_j} H(n_x) + H_2(X) \pm \text{Kinetic energy} \qquad (9a)$$

$$H_2G\,{}^1\Sigma_g^+ + H_2\,{}^1\Sigma_g^+ \xrightarrow{k_\ell} H_2(n_y) + H_2(Y) \pm \text{Kinetic energy} \qquad (9b)$$

where k_i is the respective inelastic (or super-elastic) rate constant in units of cc/molecule-sec. With this model, as shown in Ref. 3, the inclusion of collisional quenching in the decay channels yields the following equation relating S to gas density N

$$S = \frac{\omega}{4\pi} \cdot \left(\frac{I}{e}\right) \cdot L \cdot s(\lambda) \cdot \sigma_{gi} \cdot A_{ij}\,\tau_i \cdot N/(1 + k_i \cdot \tau_i \cdot N) \qquad (10)$$

where τ_i is the radiative lifetime of the ith state, H(n = 3, 4, 5) or $H_2G\,{}^1\Sigma_g^+$ in this case. One sees that S is no longer linear with respect to the density N of $H_2\,{}^1\Sigma_g^+$, but rather the slope of S versus N is a decreasing function of N, S eventually becoming insensitive to increases in number density, and thereby becoming unsuited for flow-field diagnostic measurements of local gas density.

From Eq. (10) it is seen that measurement of S as a function of gas number density N provides an experimental determination of $k_i\tau_i$ and therefore k_i, if the radiative lifetime of the radiating state is known. Equation (10) can be written as

$$N/(S/I) = \frac{1}{C}(1 + k_i\,\tau_i\,N) \qquad (11)$$

where $C = \frac{\omega}{4\pi} \cdot \frac{L}{e} \cdot s(\lambda) \cdot \sigma_{gi} \cdot A_{ij} \cdot \tau_i$ and is a constant for the measurement. The ratio of the slope to the intercept of N/(S/I) versus N therefore yields $k_i \cdot \tau_i$, or the quenching rate constant k_i.

The quenching rate constant k_i may be expressed in terms of a quenching cross section $\sigma_{in}^2(i)$ using the relation (Ref. 9)

$$k_i = \sigma_{in}^2(i) \cdot \left(\frac{8R\,T}{\pi M}\right)^{1/2} \qquad (12)$$

where R is the universal gas constant, T is the gas temperature, and M is the reduced mass of the colliding pair of species. As shown in Ref.7, the assumptions required for derivation of Eq. (12) include (a) a Maxwell-Boltzmann distribution of molecular velocities, (b) uniform gas spatial distribution, (c) hard-sphere binary-collision process, and (d) zero activation energy for the collisional transfer.

Using the same assumptions one can write the elastic rate constant $k_i(el)$ as

$$k_i(el) = \sigma^2_{el}(i)(8RT/\pi M)^{1/2}$$

where $\sigma^2_{el}(i) = \pi d^2_{ij}$ and the effective collision idameter is

$$d_{ij} = \frac{1}{2}(d_i + d_j)$$

where d_i and d_j are the collision diameters of species i and j, respectively.

One can now obtain the average inelastic transition probability per collision for state i, vix.,

$$P_i = k_i/k_i(el) = \sigma^2_{in}(i)/\sigma^2_{el}(i)$$

thereby obtaining information concerning the efficiency of the collisional process.

SECTION II
EXPERIMENTAL APPARATUS

2.1 ELECTRON BEAM SOURCE

The high energy beam of electrons is provided by a modified TV-type electron gun with magnetic focusing and deflection as shown in Fig. 3 and is essentially the same as that described in Refs. 2 and 3. The electron beam energy was 40 kev with the collision chamber grounded. Sulfur hexafluoride gas was used for pressurization of high voltage controls, including the lead wires of the gun, to eliminate arcing and corona phenomena, and operation has been achieved at accelerating voltages in excess of 60 kev with the present system. The gun system is maintained at pressures less than 10^{-5} torr using two-stage differential pumping, and the beam is injected into the outer scattering cell through a 1-mm (0.040-in.) orifice. The electron source provides in the excit-

ation region typical beam currents of approximately 1.25 ma at 40-Kev energy, and this represented 50 to 75 percent of the cathode emission current. After traversal of the gas sample the current was collected by a water-cooled, copper Faraday cup coated with colloidal graphite to suppress secondary emission. Furthermore, the collector was designed to minimize the effects of secondary emission by requiring multiple electron-collector collisions in order to re-enter the excitation region.

2.2 COLLISION CHAMBER AND VACUUM SYSTEM

The collision chamber is shown in Fig. 4 in more detail, and it is seen that the gas flow occurs within an annular water-cooled liner which is contained within--and exhausts into--the main collision chamber. As shown in Fig. 3, pumping is provided by a 4-in. oil diffusion pump and two ring-jet pumps which are backed by a Stokes mechanical roughing pump. The gas entering the flow tube is precooled and enters the annular liner as slug flow. The length of the liner was chosen so that the distance from the entrance of the liner to the point of electron beam excitation was in excess of the laminar hydrodynamic entry length $(x/D)_{vel}$ required for a fully developed velocity profile, as estimated by (Ref. 10):

$$(x/D)_{vel} = Re/20 \tag{13}$$

where x is the axial distance along the tube of diameter D confining a flow with Reynolds number (Re). Fulfillment of this criterion provides a fully developed laminar Poiseuille flow at the point of electron beam excitation, thereby enabling estimates of flow velocity gradients to be made. Additionally, the thermal entry length $(x/D)_{tel}$ is given by (Ref. 10)

$$(x/D)_{tel} = Pr\,(x/D)_{vel} \tag{13a}$$

and the Prandtl number for gases is approximately 0.7; therefore, the thermal boundary layer is fully developed before reaching the point of electron beam excitation. The precooling reservoir was maintained at approximately the same temperature as the cooling annular liner. The mass flow rate of H_2 was approximately 0.5 mg/sec, and the flow tube Mach number varied from approximately 0.01 to 0.08. Therefore, the existence of radial gradients in the gas temperature must be due to frictional heating effects. An estimate of such radial gradients can be obtained by considering the well-known problem of fully developed Poiseuille flow in a circular tube of wall temperature T_o. It is easily shown that the centerline temperature T_{max} for a subsonic flow of centerline Mach

number M_{cl} is given by

$$(T_{max} - T_o)/T_{max} = (\frac{1}{4}) \left[Pr(\gamma - 1) (M_{cl})^2\right]$$

where γ is the specific heat ratio for the gas. For H_2 it is easily seen that T_{max} differs from T_o by less than 0.1 percent for Mach numbers less than 0.1, and therefore, the effect of radial temperature gradients is negligible. The temperatures of the flow tube liner and the reservoir were monitored by nine thermocouples located at various positions, including the water-cooled electron beam entrance orifice shown in Fig. 4 and the Faraday cup, and no significant gradients were present.

The chamber was pumped to a pressure of approximately 5×10^{-6} torr, and the pumping lines were purged with argon for approximately two hours to remove residual oxygen-containing air from the system. Research grade hydrogen gas was then injected into the flow system, and flow was maintained for approximately one hour before data acquisition was begun. The pressure, as measured with a calibrated MKS Baratron, was systematically increased or decreased, steady state was achieved and data recorded. This procedure was repeated until the quenching curve was sufficiently defined, as described in a following section.

2.3 OPTICAL AND ELECTRONICS DETECTION SYSTEM

Two different optical arrangements were used for data acquisition. The H_β radiation, as well as the other transitions investigated, was observed in a direction perpendicular to both the electron beam and the gas flow as Fig. 5 shows. The H_β radiation was collected by a lens of 5-cm diameter and 250-mm focal length, passed through a Dove prism to ensure complete collection of the radiation and focused onto the entrance slit of a 3/4-m Spex monochromator with a 1180-gm/mm, 5000-Å blaze grating. The output at the exit slit was detected by a gaseous-nitrogen-cooled photomultiplier tube, and the data were acquired using both an EMI 6256B and an RCA 7265 tube. The spectral bandwidth of the H_β data was a minimum of 4 Å and a maximum of 8 Å for the series of measurements. The photomultiplier output was processed by a pulse amplifier, discriminator, and counter, the last of which recorded the total number of photon counts over a specified counting interval. Figure 6 shows the electronic system used for data acquisition. Linearity of the system has been verified using the variation of output signal as a function of beam current at constant density for the first negative system of N_2^+. The observed photon emission rate was always sufficiently low that no dead-time corrections were required of the 20-MHz counter output. An additional precaution taken to ensure repeatability of the data

was operation of the discriminator at such a voltage that small changes in the cooled photomultiplier temperature had no effect on the signal-to-noise ratio of the output. The measurements of the H_α, H_γ, and H_2 $G \longrightarrow B$ transition were made with identical apparatus and precautions except that a 1/4-m Jarrell-Ash monochromator with diffraction gratings of 1180 gm/mm and 3000- and 6000-Å blazes was aligned so that the length of the entrance slit was perpendicular to the direction of the beam and the Dove prism was removed. The magnification of the optical system was one half, and the monochromator slits were 250 μm by 20 mm, thereby giving a 40-mm image of the slit at the position of the electron beam. The spectral bandwidth was approximately 8 Å in all cases.

SECTION III
EXPERIMENTAL RESULTS AND ANALYSIS

3.1 EXPERIMENTAL RESULTS

To ensure the absence of spectral impurities a broad wavelength scan of the 3000- to 6500-Å spectral region was periodically performed using a PAR® HR-8 lock-in amplifier, and Fig. 7 shows a typical strip-chart recording.

The variation of the photon emission rate of the H_α, H_β, H_γ, and H_2 (4634 Å) was observed as a function of H_2 gas density, and the photon emission rate in each case was normalized to unit beam current. Because data were acquired for a range of beam current values, the linearity of the photon emission rate with beam current was verified for each of the systems studied, and Fig. 8 shows a typical result for the H_α system. The pressure range observed varied with the radiating specie but was typically 100 μ Hg to 2 torr at an average gas temperature of 292°K. Figure 9 shows a typical result of the current-normalized photon emission rate of the H_β system versus gas pressure, and it is seen that the nonlinearity becomes evident at 250 μ Hg. Additionally, it should be noted that if collisional quenching is neglected and the low density linear dependence of the photon emission rate is extrapolated to high density for the purpose of performing a flow-field measurement of local H_2 density, at 400 μ Hg there exists an error exceeding 20 percent and 30 percent at 800 μ Hg.

The photon emission rate data of the H_α, H_β, H_γ, and H_2 $G \longrightarrow B$ systems as a function of $H_2 X^1\Sigma_g^+$ number density were plotted according to Eq. (11), and typical results are shown in Figs. 10 through 13 for the respective systems.

A computer calculation of the least-squares fit of the data to an equation of the form of Eq. (11) was performed, and the individual measured values of $k_i\tau_i$ were obtained as well as the statistical error σ_i of the fit to the data (Ref. 11). The weighted mean value of k_i, $\bar{k}_i$, of the J_i individual determinations of a given transition, as well as the uncertainty σ_M of the set of data were determined using (Ref. 11)

$$\bar{k}_i = \sum_{j=1}^{J_i} k_i(j)/\sigma_i^2(j) / \left[\sum_{j=1}^{J_i} 1/\sigma_i^2(j)\right] \tag{14}$$

and

$$1/\sigma_{Mi}^2 = \sum_{j=1}^{J_i} 1/\sigma_i^2(j) \tag{15}$$

and the values obtained are listed in Table II. The values of $2\sigma_{Mi}$ listed in Table II are the approximate 95-percent confidence level values.

For the Balmer series the radiative, field-free lifetimes were obtained from Ref. 12 and used to obtain the quenching rates $\bar{k}_i$ of each atomic state, and these values are given in Table II. The $H_2G^1\Sigma_g^+$ lifetime was assumed to be 10 nsec merely for the purpose of comparison, and its value of $\bar{k}_i$ is shown in Table II.

Using the hard-sphere binary-collision model representation and Eq. (12), the inelastic cross section $\sigma_{in}^2(i)$ for each excited state was calculated and listed in Table II.

3.2 ANALYSIS

3.2.1 Atomic Hydrogen De-Excitation

The deactivation cross-section experimental results which are shown in Table II clearly demonstrate a trend of decreasing cross section with increase of electronic excitation energy of the hydrogen atom. Since the Bohr radius r of the excited electron of a hydrogen atom varies as

$$r = n^2 a_o$$

one would intuitively expect the elastic cross section or the collision rate of H_2 with H(n) to increase as the excitation energy increased (Ref. 13). Therefore, it is obvious that the deactivation efficiency of the H(n),

$H_2X^1\Sigma_g^+(v = 0)$ collision decreases as the atomic electronic excitation energy increases. Such a variation in the behavior of the deactivation cross section may be due to a resonance effect in the energy transfer mechanism; i. e., the de-excitation process found to be most efficient is that process which minimizes the amount of energy ΔE to be transferred either to or from the translational mode, all other factors being equal. Therefore, one is led to consider possible energy transfer mechanisms from the H(n = 3, 4, 5) states to the H_2 molecule for which a minimum ΔE is required.

Considering first the n = 3 state the following deactivation schemes represent processes for which (1) ΔE is minimized and/or (2) the transition is allowed according to the optical selection rules. It will be seen that the transitions are of two general types: (1) electronic-to-electronic energy transfer and (2) electronic-to-vibrational energy transfer (Ref. 14).

(1) Electronic-to-Electronic Energy Transfer

$$H(n=3) + H_2X^1\Sigma_g^+(v=0) \longrightarrow H(n=1) + H_2B^1\Sigma_u^+(v=5) + 0.13 \text{ ev} \quad (16a)$$

which can be written as

$\left[(H)_3^1,\ (H_2)_{X0}^{B5}\right]$ + 0.13 ev, where subscripts represent the initial state and superscripts the final state. For H_2, Xv represents $H_2X^1\Sigma_g^+(v)$ and Bv represents $H_2B^1\Sigma_u^+(v)$. The energy +0.13 ev represents an exoergic transfer of 0.13 ev,

$$\left[(H)_3^1,\ (H_2)_{X0}^{B6}\right] \text{ -0.011 ev} \quad (16b)$$

The vibrational energy eigenvalues of Dieke (Ref. 15) are used for the $H_2B^1\Sigma_u^+ \longrightarrow H_2X^1\Sigma_g^+$ transition.

(2) Electronic-to-Vibrational Energy Transfer

$$\left[(H)_3^2,\ (H_2)_{X0}^{X1}\right] + 1.372 \text{ ev} \quad (16c)$$

$$\left[(H)_3^2,\ (H_2)_{X0}^{X2}\right] + 0.886 \text{ ev} \quad (16d)$$

$$\left[(H)_3^2,\ (H_2)_{X0}^{X3}\right] + 0.429 \text{ ev} \quad (16e)$$

$$\left[(H)_3^2,\ (H_2)_{X0}^{X4}\right] + 0.001 \text{ ev} \quad (16f)$$

$$\left[(H)_3^2,\ (H_2)_{X0}^{X5}\right] - 0.397 \text{ ev} \quad (16g)$$

and

$$\left[(H)_3^2,\ (H_2)_{X0}^{X6}\right] - 0.762 \text{ ev} \tag{16h}$$

The electronic excitation processes of Eqs. (16a) and (16b) were selected so that (1) excitation transfer is g ⟶ u allowed, (2) the Franck-Condon rule is obeyed, and (3) ΔE is minimized. The electronic-to-vibrational transfer cases of Eqs. (16c) through (16h) show that for ΔE to be minimized the $H_2X^1\Sigma_g^+$ molecule must undergo a multiquanta, $\Delta v = 4$, transition.

In a similar manner one can arrive at the following possibilities for deactivation of the H(n = 4) and H(n = 5) states:

$$\left[(H)_4^1,\ (H_2)_{X0}^{B10}\right] + 0.12 \text{ ev} \tag{17a}$$

$$\left[(H)_4^1,\ (H_2)_{X0}^{B11}\right] - 0.0035 \text{ ev} \tag{17b}$$

$$\left[(H)_4^2,\ (H_2)_{X0}^{X5}\right] + 0.265 \text{ ev} \tag{17c}$$

$$\left[(H)_4^2,\ (H_2)_{X0}^{X6}\right] - 0.010 \text{ ev} \tag{17d}$$

$$\left[(H)_4^3,\ (H_2)_{X0}^{X1}\right] + 0.144 \text{ ev} \tag{17e}$$

$$\left[(H)_4^3,\ (H_2)_{X0}^{X2}\right] - 0.342 \text{ ev} \tag{17f}$$

and

$$\left[(H)_5^1,\ (H_2)_{X0}^{B13}\right] + 0.067 \text{ ev} \tag{18a}$$

$$\left[(H)_5^1,\ (H_2)_{X0}^{B14}\right] - 0.045 \text{ ev} \tag{18b}$$

$$\left[(H)_5^3,\ (H_2)_{X0}^{X1}\right] + 0.451 \text{ ev} \tag{18c}$$

$$\left[(H)_5^3,\ (H_2)_{X0}^{X2}\right] - 0.005 \text{ ev} \tag{18d}$$

$$\left[(H)_5^3,\ (H_2)_{X0}^{X3}\right] - 0.492 \text{ ev} \tag{18e}$$

$$\left[(H)_5^4,\ (H_2)_{X0}^{X1}\right] - 0.210 \text{ ev} \tag{18f}$$

$$\left[(H)_5^4,\ (H_2)_{X0}^{X2}\right] - 0.636 \text{ ev} \tag{18g}$$

Considering the H(n = 3) transitions and specifically Eqs. (16a) through (16h), it is seen that the magnitude of the energy imbalance ΔE as a function of vibrational quantum number change Δv is sharply peaked

for $\Delta v = 4$. However, it is well known that multiquanta processes are inherently inefficient (Ref. 16), and consequently one must conclude that the deactivation process of Eq. (16f) is unlikely so long as no potential curve crossing occurs. One is left with the processes of Eqs. (16a) and (16b) as likely deactivation mechanisms.

For the possible H(n = 4) deactivation mechanisms, the deactivation paths of Eqs. (17c) and (17d) are both multiquanta jumps for the $H_2X^1\Sigma_g^+(v = 0)$ molecule and are, therefore, unlikely. Equation (17f) indicates a double quantum jump of the H_2 molecule which is endoergic by 0.342 ev and is negligible, since on the basis of hard-sphere, Maxwell-Boltzmann kinetic theory, only approximately one in every 10^6 collisions possesses sufficient translational energy to provide the 0.34-ev energy deficiency. One is left, therefore, with the process of Eq. (17e) which is a single quantum jump process and is exoergic by 0.144 ev. The electronic-to-electronic processes of Eqs. (17a) and (17b) are both Franck-Condon allowed and possible from the standpoint of the endoergicity of the decay path. Therefore, for the deactivation of the H(n = 4) state, one has the possible decay paths represented by Eqs. (17a), (17b), and (17e).

For the deactivation of the H(n = 5) state, similar reasoning narrows the possible decay paths to those represented by Eqs. (18a), (18b), (18c), and (18d).

From the above considerations the suggested possible deactivation mechanisms for the H(n = 3, 4, 5) states are:

for the H(n = 3),

$$\left[(H)_3^1,\ (H_2)_{X0}^{B5}\right] + 0.13 \text{ ev} \tag{16a}$$

$$\left[(H)_3^1,\ (H_2)_{X0}^{B6}\right] - 0.011 \text{ ev} \tag{16b}$$

for H(n = 4),

$$\left[(H)_4^1,\ (H_2)_{X0}^{B10}\right] + 0.12 \text{ ev} \tag{17a}$$

$$\left[(H)_4^1,\ (H_2)_{X0}^{B11}\right] - 0.0035 \text{ ev} \tag{17b}$$

$$\left[(H)_4^3,\ (H_2)_{X0}^{X1}\right] + 0.144 \text{ ev} \tag{17e}$$

and for H(n = 5),

$$\left[(H)_5^1,\ (H_2)_{X0}^{B13}\right] + 0.067 \text{ ev} \tag{18a}$$

$$\left[(H)_5^1,\ (H)_{X0}^{B14}\right] - 0.045 \text{ ev} \tag{18b}$$

$$\left[(H)_5^3,\ (H_2)_{X0}^{X1}\right] + 0.451 \text{ ev} \tag{18c}$$

$$\left[(H)_5^3,\ (H_2)_{X0}^{X2}\right] - 0.005 \text{ ev} \tag{18d}$$

It should be noted that in principle, processes of the type represented by Eqs. (17e), (18c), and (18d) are experimentally detectable for they represent collisional cascading processes. If such processes are present both the pressure variation of the photon emission rate S and the value of the absorption coefficient obtained from a simultaneous measurement of either the H(n = 3) ⟶ H(n = 4) or H(n = 4) ⟶ H(n = 5) transitions should so indicate. However, accurate interpretation of the results of such measurements requires knowledge of the electron-molecule excitation cross section of the H(n = 3, 4, 5) states at 40 kev, and such data do not at present exist. It can only be said that within the precision of the current measurement, collisional cascading effects were not observed for the H_β and H_α quenching curves.

If one assumes that the quenching of the H(n = 3, 4, 5) states is represented by processes described by Eqs. (16a), (16b), (17a), (17b), and (18a), (18b), respectively, on the assumption of no potential curve crossing and an interaction potential factorable in the electron coordinates of the atom and molecule, the use of electric dipole selection rules should provide a first approximation for calculation of the cross section. Neglecting constants and the factor representing efficiency of conversion of electronic to translational energy, the deactivation cross section $\sigma^2(ij)$ for the i to j transition can be written as

$$\sigma^2(ij) \propto A_{ij}\, q_{vv'} \tag{19}$$

where $q_{vv'}$ represents the Franck-Condon factor of the $H_2X^1\Sigma_g^+(v)$ to $H_2B^1\Sigma_u^+(v')$ excitation. Therefore, using values of $q_{vv'}$ given by Spindler (Ref. 17), one finds, using Eq. (19),

$$\sigma^2(3\ 1) : \sigma^2(4\ 1) : \sigma^2(5\ 1) = 1 : 0.18 : 0.05 \tag{20}$$

The experimental results of Table II give

$$\sigma^2(3\ 1) : \sigma^2(4\ 1) : \sigma^2(5\ 1) = 1 : 0.42 : 0.12 \qquad (21)$$

which yields order-of-magnitude agreement with Eq. (20).

3.2.2 Molecular Hydrogen

Because the emitted radiation detected at 4634 Å is only tentatively identified as arising from the $H_2G^1\Sigma_g^+ \longrightarrow H_2B^1\Sigma_u^+$ transition, a nominal value of 10 msec was assumed for the radiative lifetime, yielding an inelastic cross section of 38 $Å^2$ as shown in Table II. If the transition identification is correct it is felt that the assumed lifetime value may be too small by less than an order of magnitude, in which case the measured cross section quoted in Table II will be increased to a value much larger than the gas kinetic value.

SECTION IV
CONCLUSIONS

The collisional quenching of the H(n = 3, 4, 5) states by ground state H_2 is suggested as being the result of electronic-to-electronic energy transfer processes in which the H atom is deactivated to its ground electronic state and H_2 is excited to the $H_2B^1\Sigma_u^+$ state. Although there is a wide variation of quenching cross sections, as shown in Table II, it should be noted that the $k\tau$ products of the three states are of the same order of magnitude. Inasmuch as it is the $k\tau$ product rather than σ^2_{in} which determines the density variation of the electron-beam-induced fluorescense, it is seen that on the basis of quenching there is little to recommend one transition over the other, based on room temperature measurements. The molecular hydrogen transition, however, exhibits a $k\tau$ product at room temperature which is significantly less than any of the atomic transitions. However, temperature dependencies are likely to be greater for the molecular transition than for the atomic excitations produced by dissociative excitation. Further measurements investigating the temperature dependence of excitation and quenching of both the atomic and molecular transitions are required.

REFERENCES

1. Muntz, E. P. and Marsden, D. J. Rarefied Gas Dynamics II. Edited by J. A. Laurmann, Academic Press, New York, 1963.
2. Williams, W. D., Hornkohl, J. O., and Lewis, J. W. L. "Electron Beam Probe for a Low Density Hypersonic Wind Tunnel." AEDC-TR-71-61 (AD727004), July 1971.
3. Norman, Wendell, Kinslow, Max, and Lewis, J. W. L. "Experimental Study of Simulated High Altitude Rocket Exhaust Plumes." AEDC-TR-71-25 (AD726555), July 1971.
4. Massey, H. S. W., Burhop, E. H. S., and Gilbody, H. B. Electronic and Ionic Impact Phenomena, Volume II. Oxford at the Clarendon Press, 1969.
5. Vroom, D. A. and de Heer, F. J. "Production of Excited Atoms by Impact of Fast Electrons on Molecular Hydrogen and Deuterium." Jour. Chem. Phys., Vol. 50, 1969, pp. 580-590.
6. Sharp, E. T. "Potential Energy Curves for Molecular Hydrogen and its Ions." Atomic Data, Vol. 2, 1971, pp. 119-169.
7. Herzberg, G. Molecular Spectra and Molecular Structure I. Spectra of Diatomic Molecules. D. Van Nostrand Company, Inc., Princeton, New Jersey, 1964.
8. Kruithof, A. A. and Ornstein, L. S. "Anregung Einiger Spektralinien des Wasserstoffmoleküls durch Electronstoss." Physica, Vol. 2, 1935, pp. 611-617.
9. Johnston, H. S. Gas Phase Reaction Rate Theory. The Ronald Press Company, New York, 1966.
10. Kays, W. M. Convective Heat and Mass Transfer. McGraw-Hill Book Company, New York, 1966.
11. Beers, Y. Introduction to the Theory of Error. Addison-Wesley Publishing Company, Inc., Reading, Massachusetts, 1953.
12. Wiese, W. L., Smith, M. W., and Glennon, B. M. Atomic Transition Probabilities, Vol. I. NSRDS-NB4, U. S. Government Printing Office, Washington, D. C., 1966.
13. Hirschfelder, J. O., Curtiss, C. F., and Bird, R. B. Molecular Theory of Gases and Liquids. John Wiley and Sons, Inc., New York, 1954.

14. Gaydon, A. G. and Hurle, I. R. The Shock Tube in High-Temperature Chemical Physics. Reinhold Publishing Corporation, New York, 1963.

15. Dieke, G. H. "The Molecular Spectrum of Hydrogen and Its Isotopes." Jour. Mol. Spec., Vol. 2, 1958, pp. 494-517.

16. Dickens, P. G., Linnett, J. W., and Sovers, O. "Collisional Energy Transfer Between Electronic and Vibrational Degrees of Freedom." Disc. Far. Soc., Vol. 33, 1962, pp. 52-60.

17. Spindler, R. J. "Franck-Condon Factors for Band Systems of Molecular Hydrogen-I." J. Quant. Spectrosc. Radiat. Transfer, Vol. 9, 1969, pp. 597-626.

APPENDIXES

I. ILLUSTRATIONS
II. TABLES

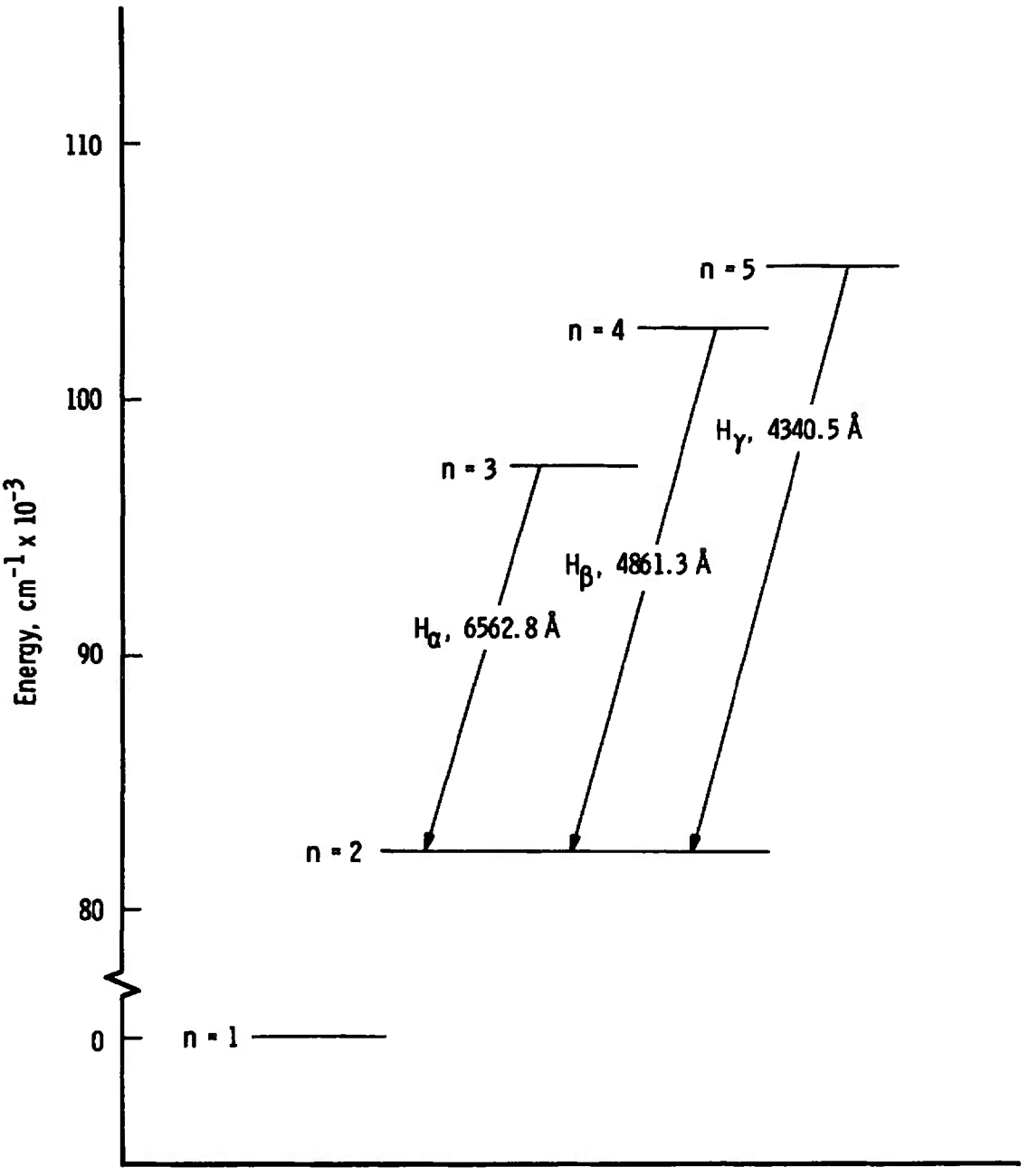

Fig. 1 Energy Level Diagram of Atomic Hydrogen

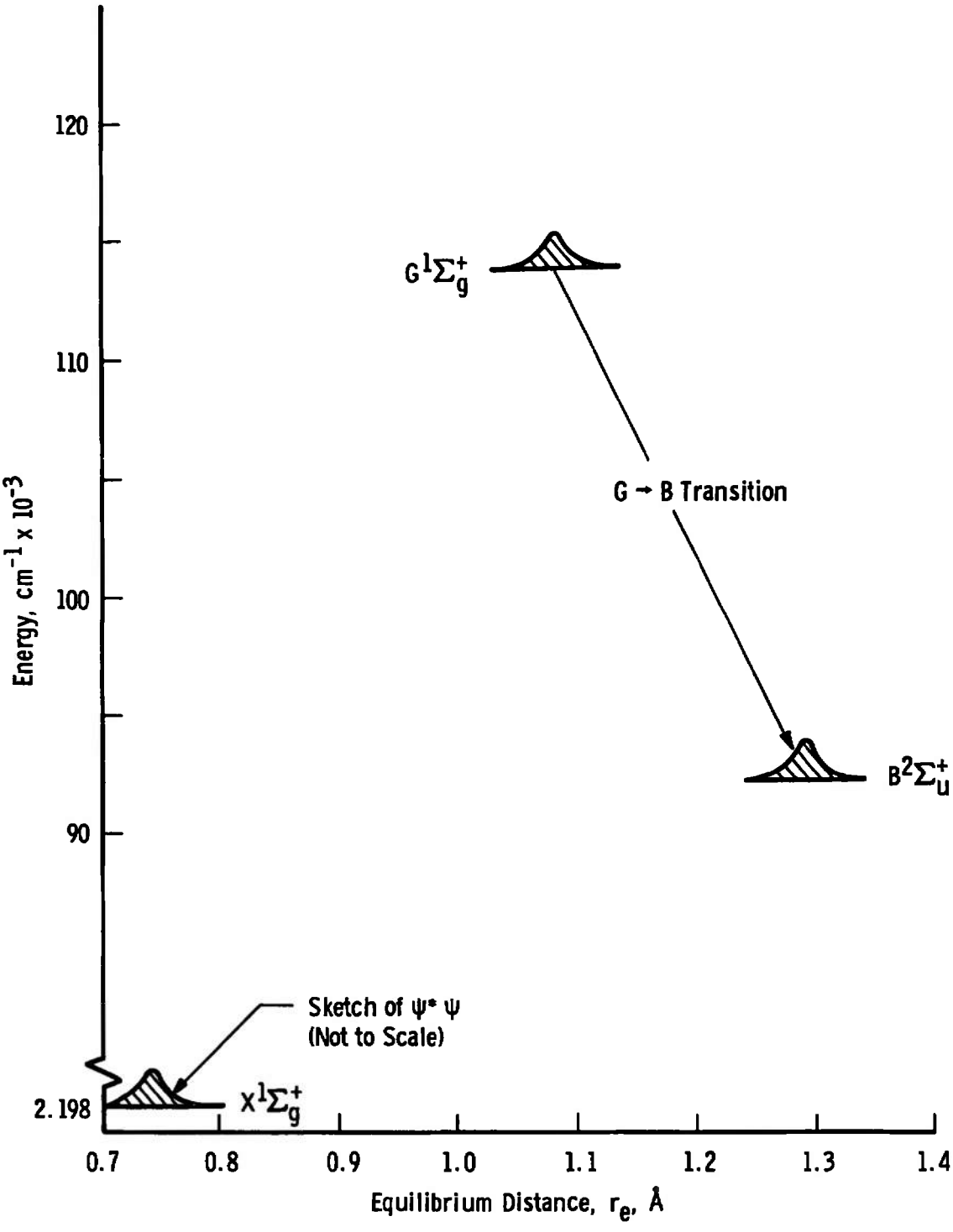

Fig. 2 Partial Electronic Energy Level Diagram of H_2

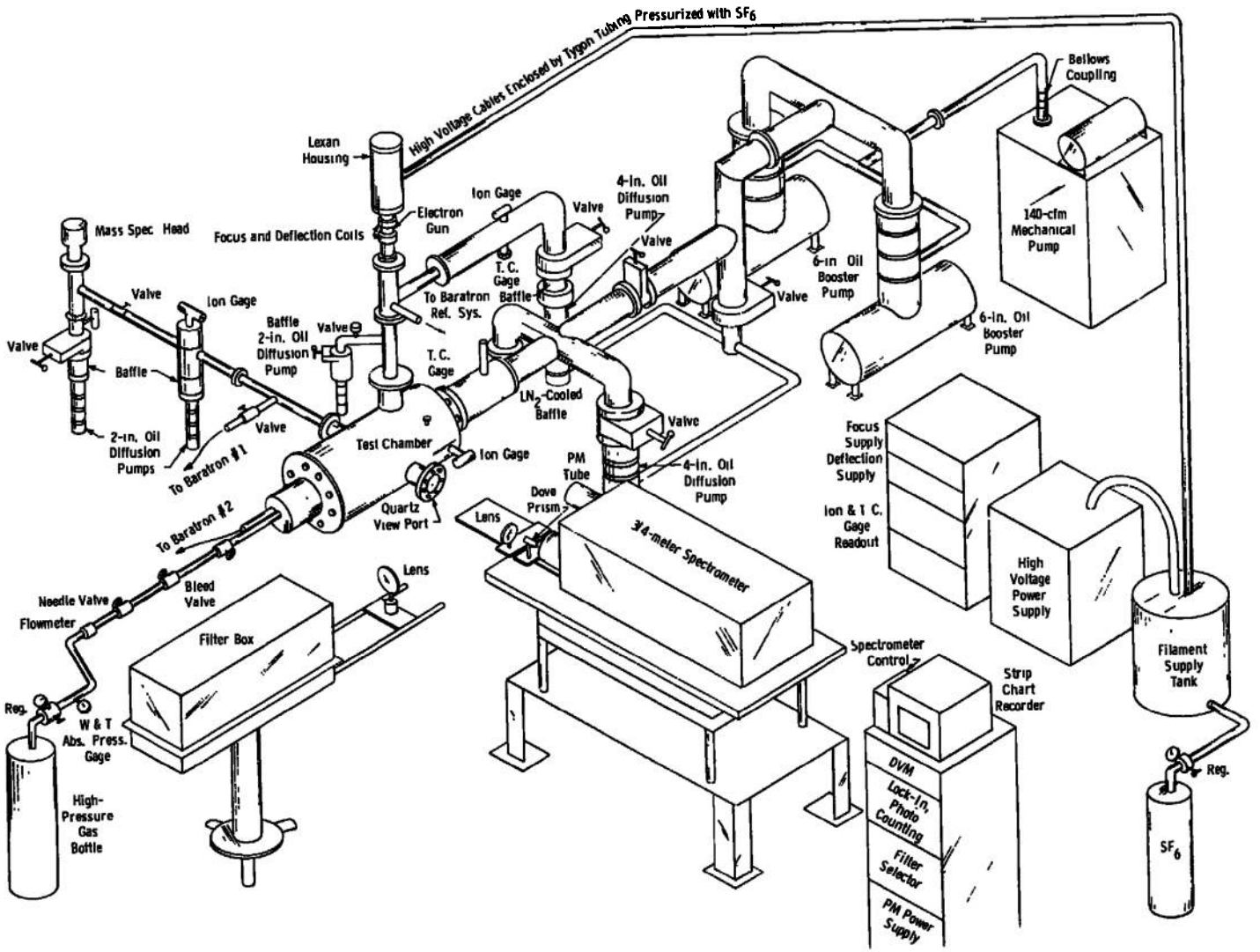

Fig. 3 Experimental System

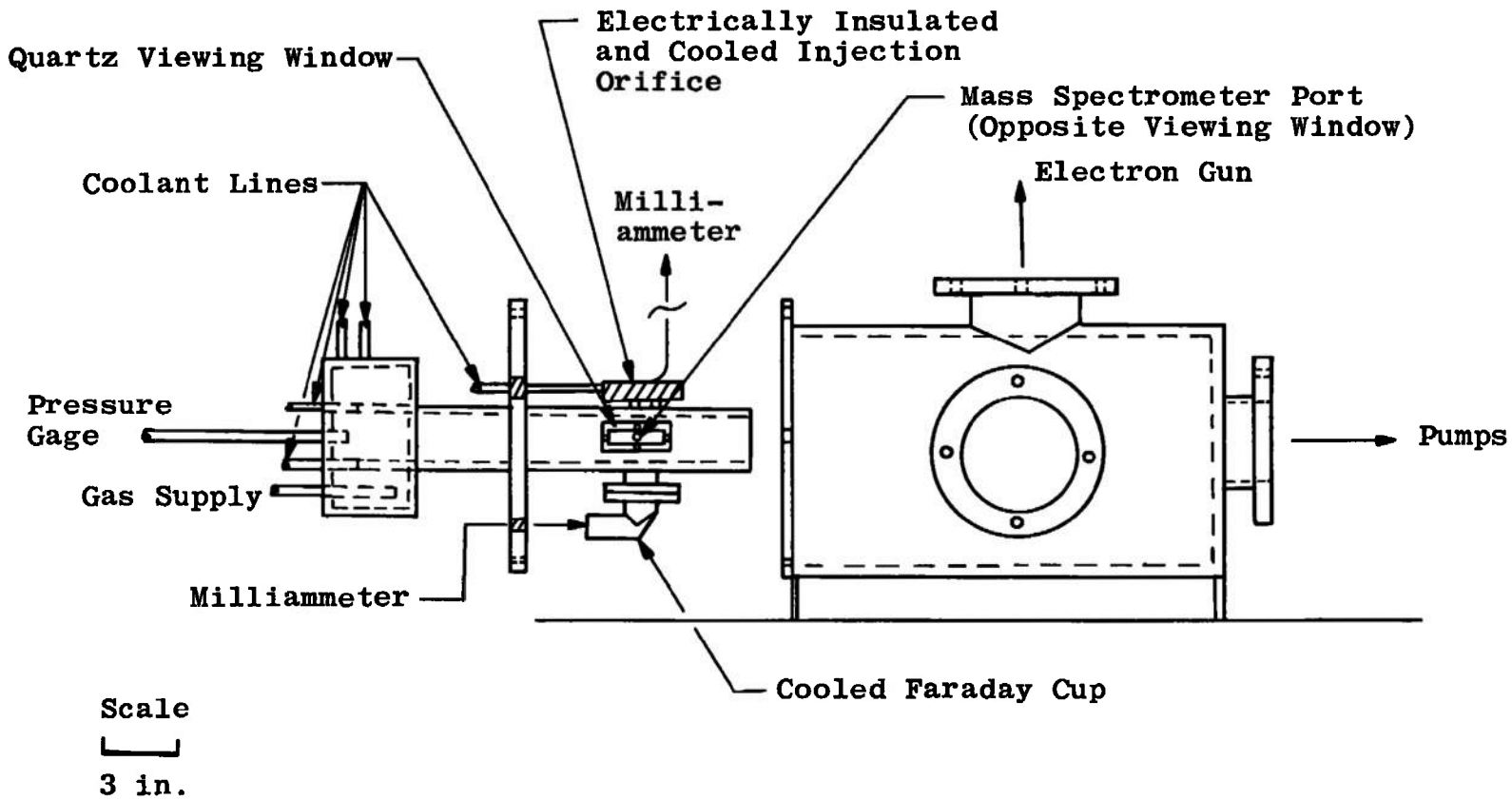

Fig. 4 Gas Flow Tube Liner

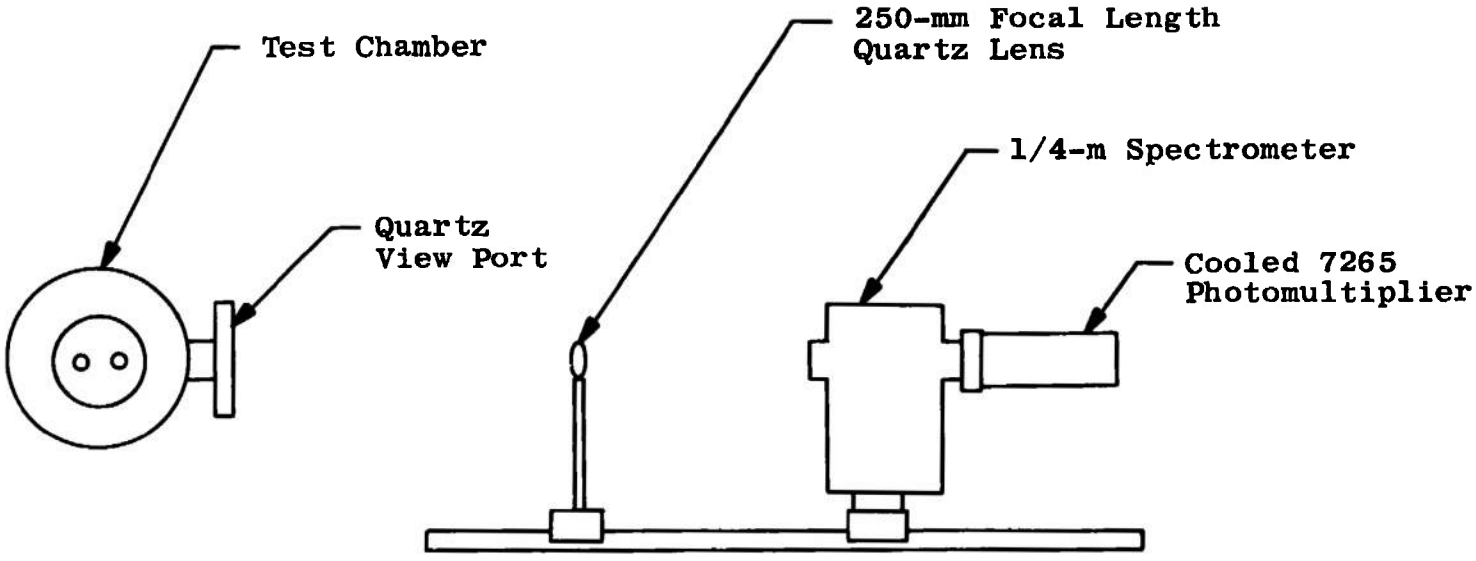

Fig. 5 Optical Arrangement

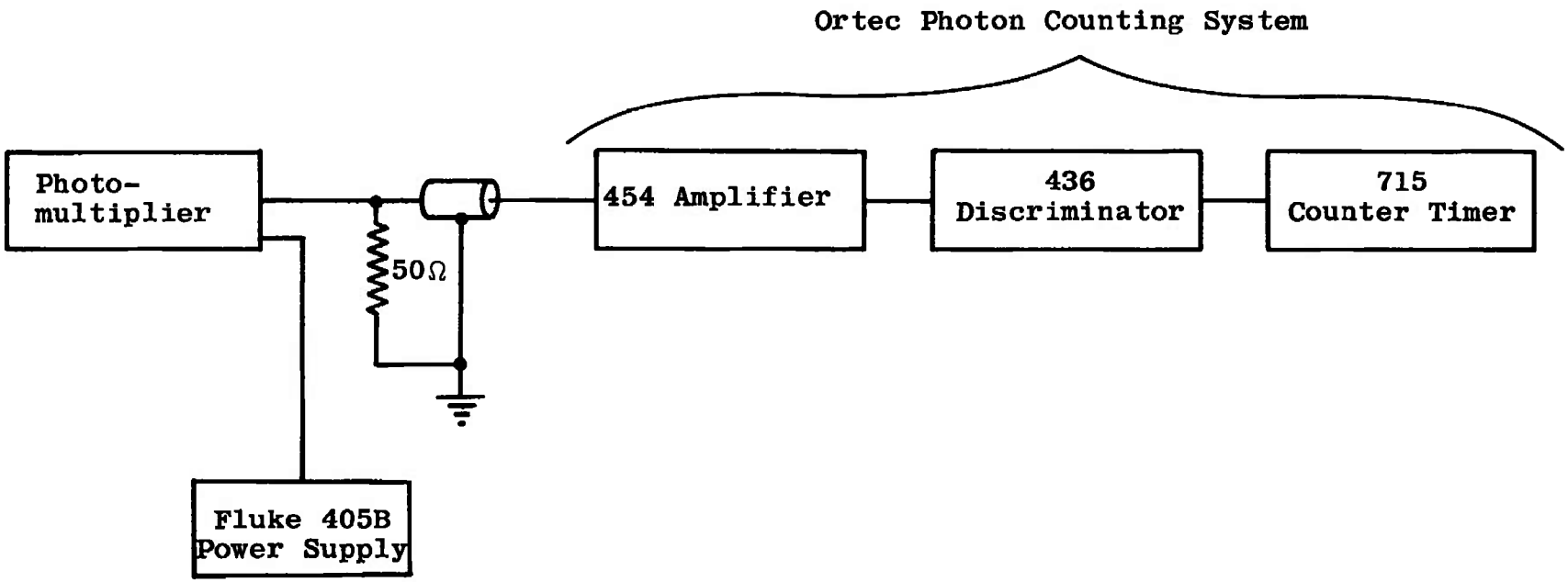

Fig. 6 Electronics System

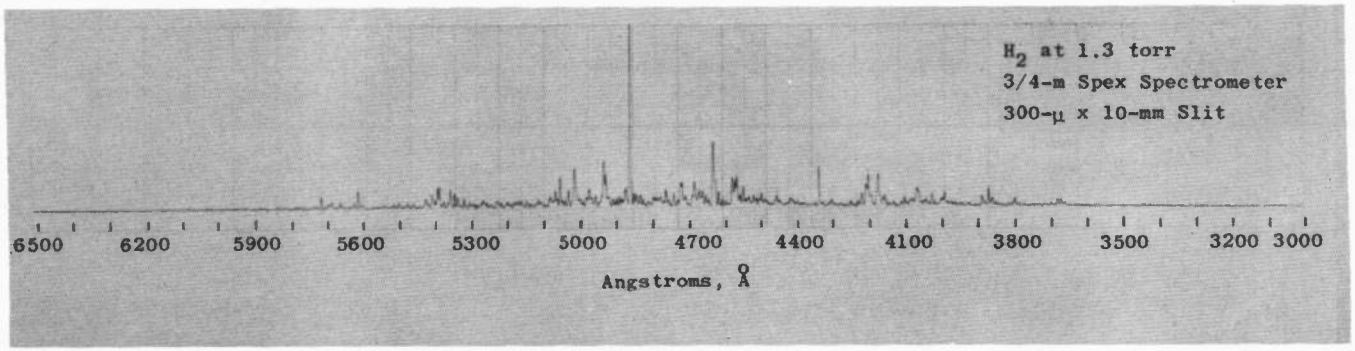

Fig. 7 Spectral Scan of Hydrogen Radiation

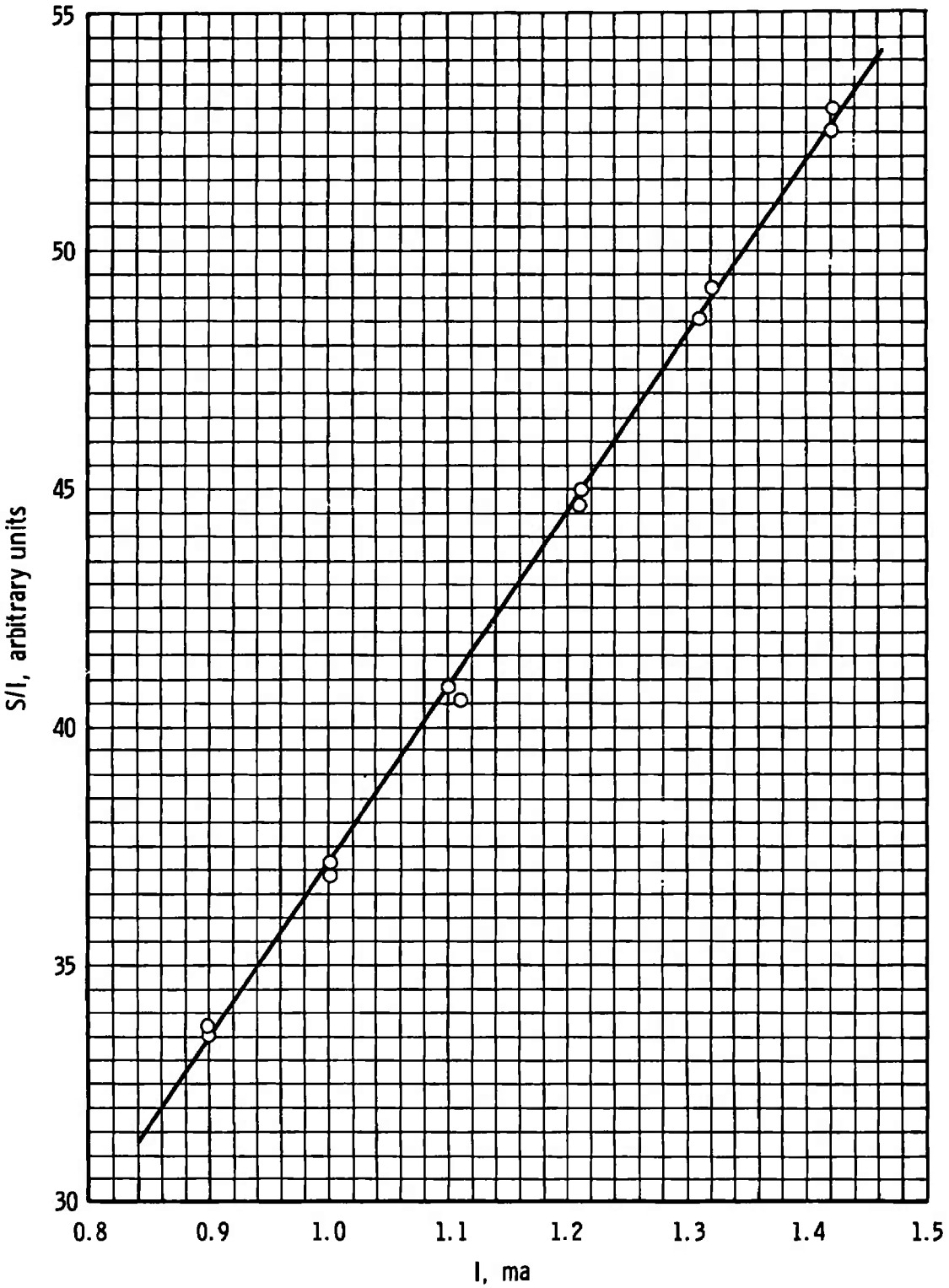

Fig. 8 H_α Photon Emission Rate versus Beam Current

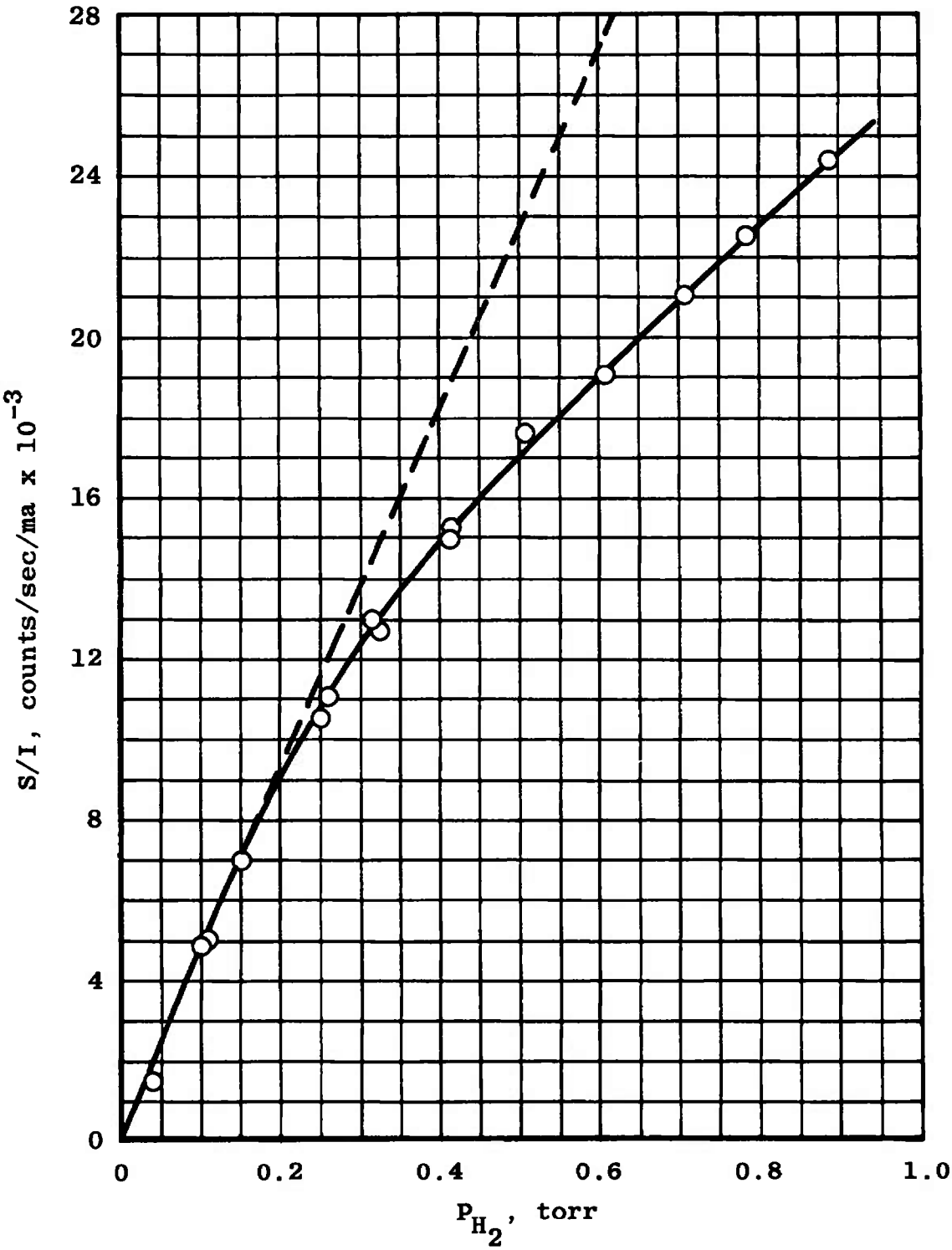

Fig. 9 S/I versus H_2 Pressure for Hβ Transition

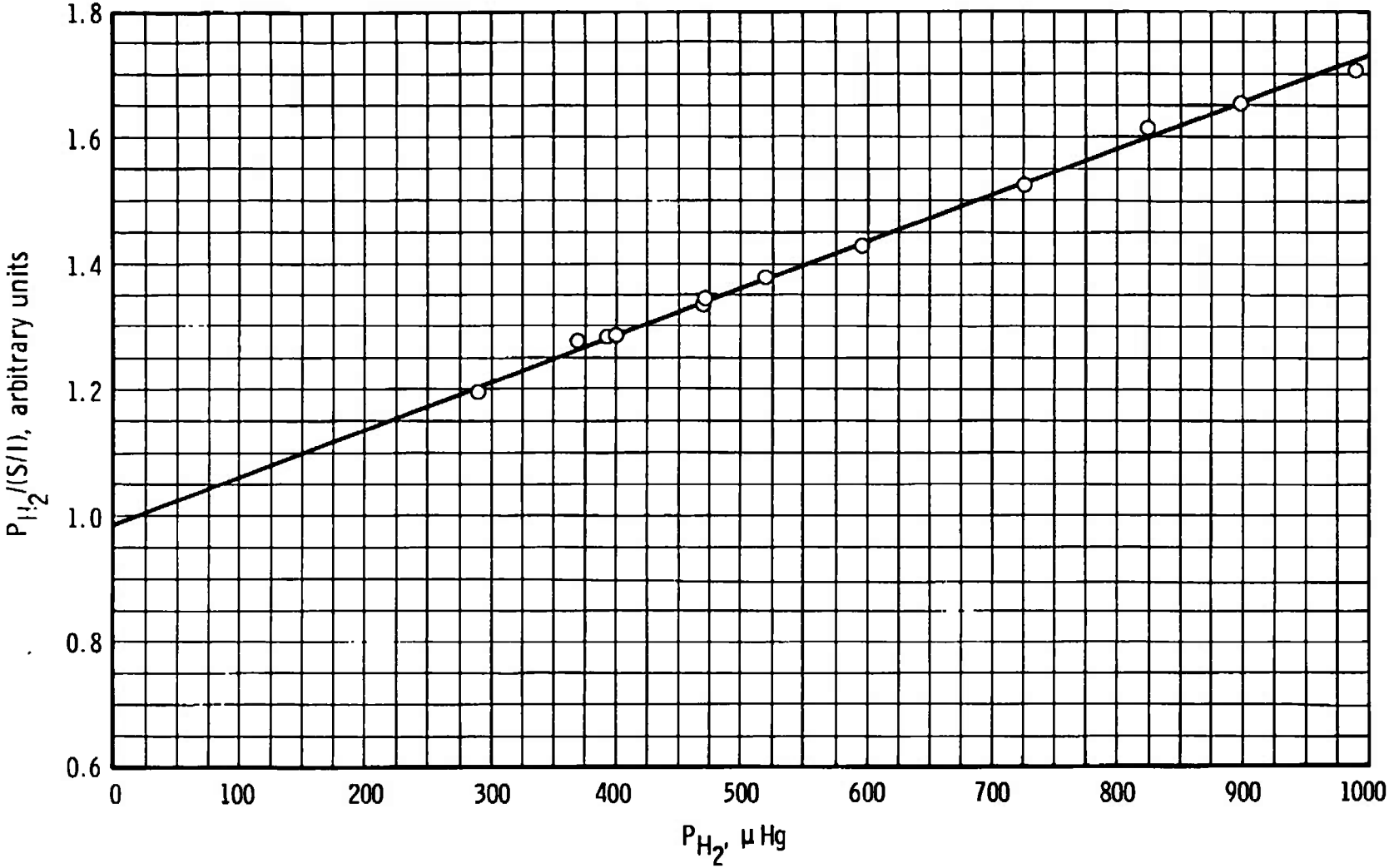

Fig. 10 Quenching Curve for H_α Transition

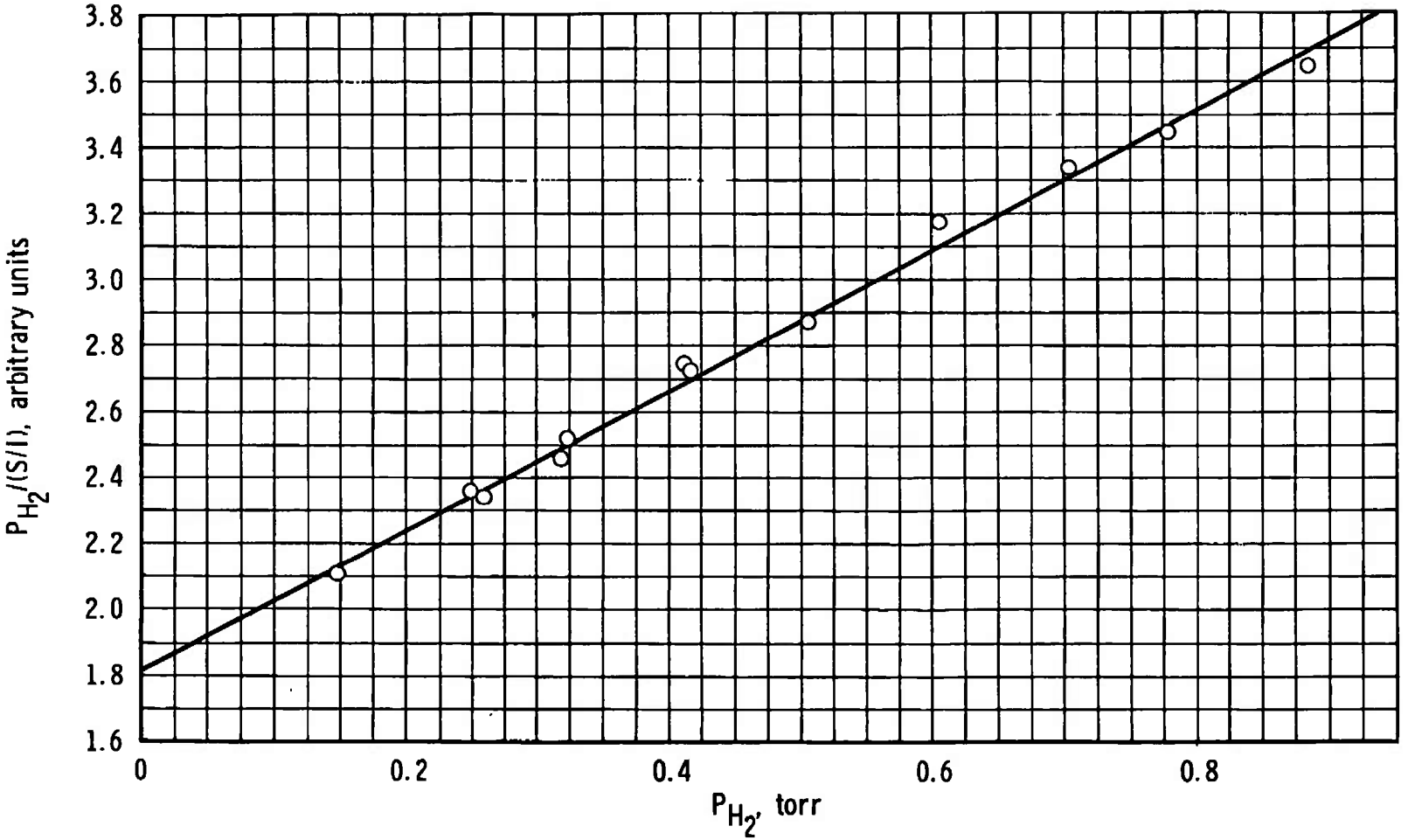

Fig. 11 Quenching Curve for Hβ Transition

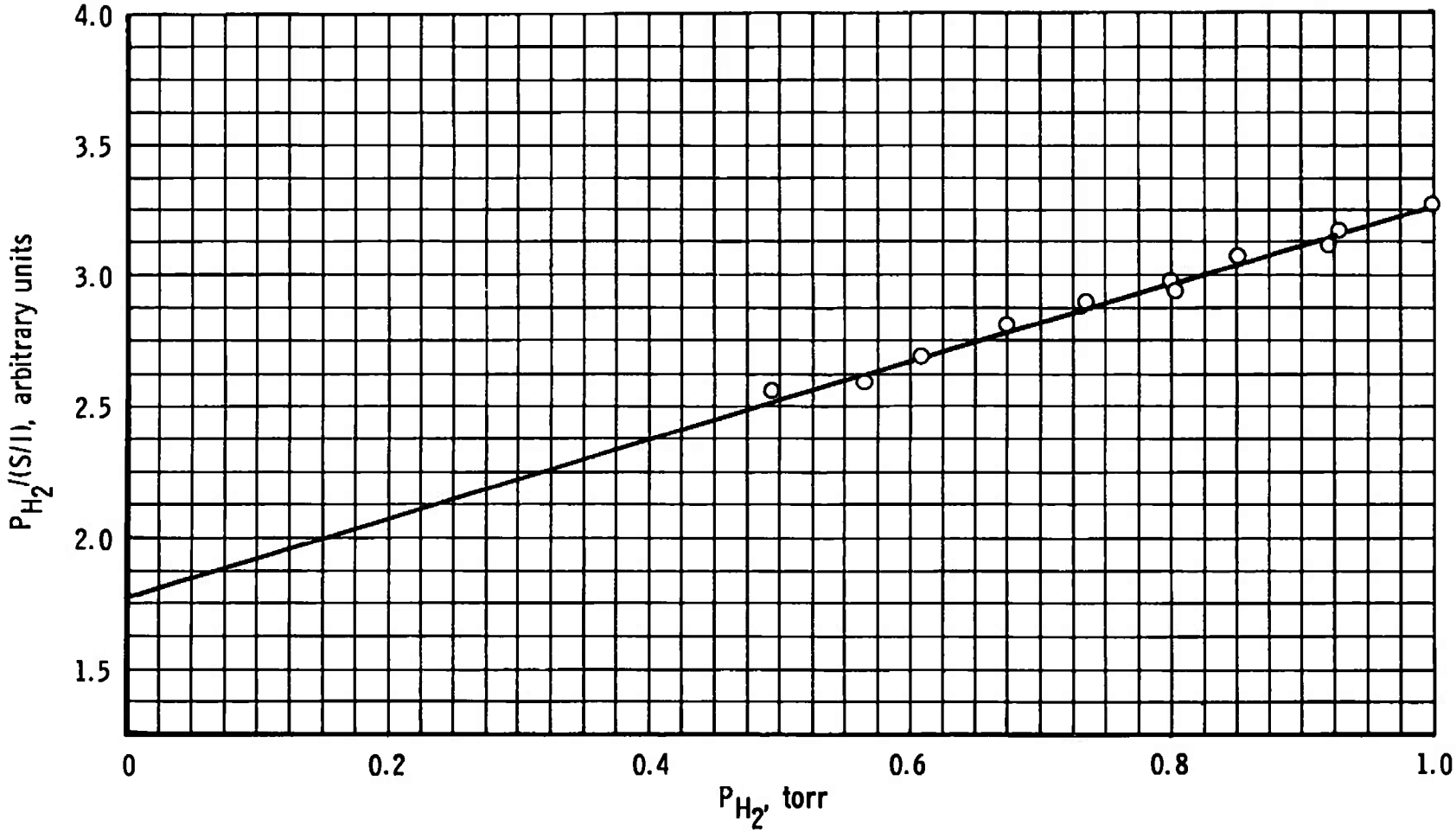

Fig. 12 Quenching Curve for H_γ Transition

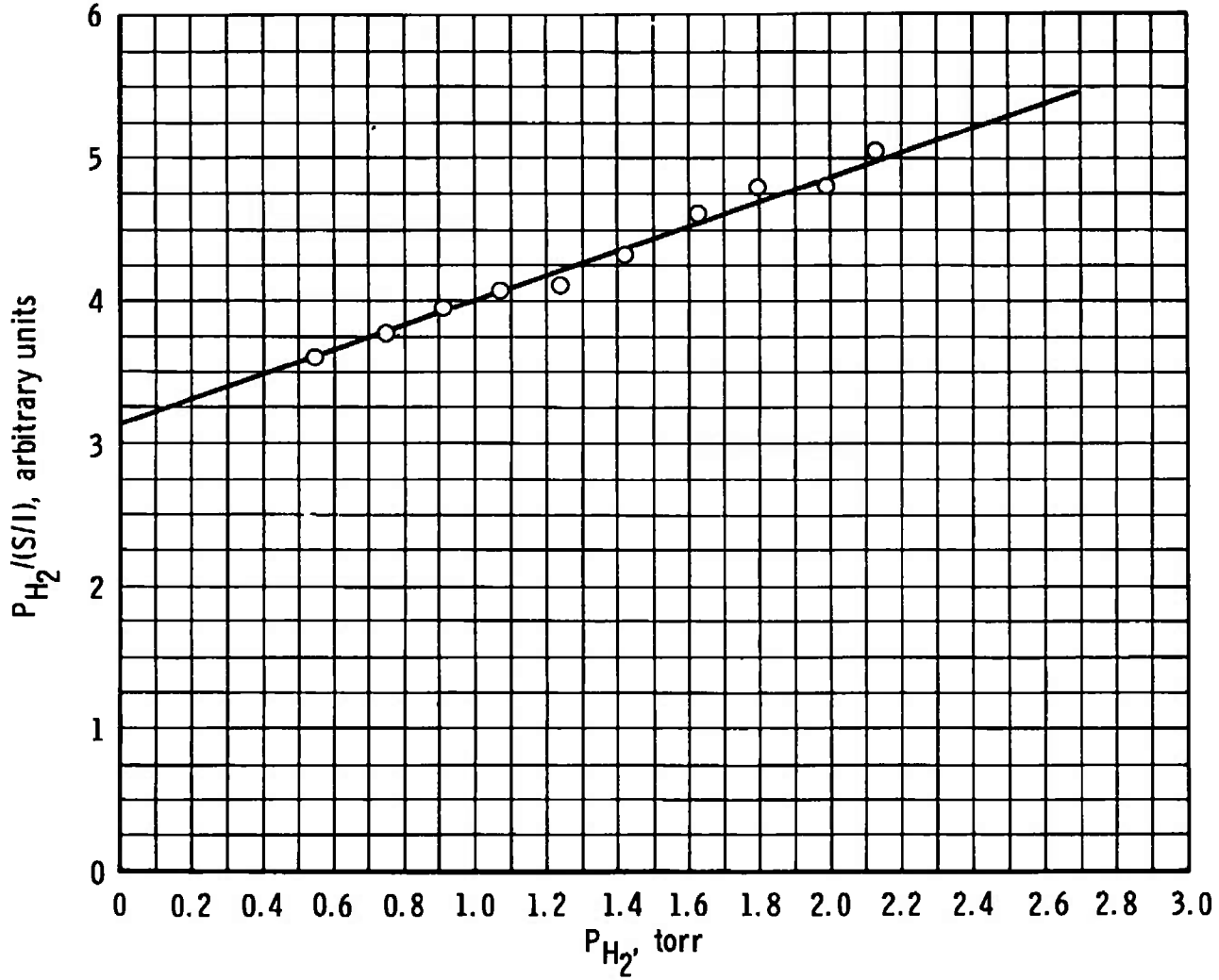

Fig. 13 Quenching Curve for H_2 (G → B) Transition

TABLE I
$H_2G^1\Sigma_g^+ \rightarrow H_2B^1\Sigma_u^+$ LINE ASSIGNMENT

λ, Å	Designation	λ, Å	Designation
4629.3	R(1)	4636.0	P(0)
4632.8	R(2)	4653.0	P(1)
4635.3	R(3)	4674.4	P(2)
4535.9	R(4)	4693.3	P(3)
4633.1	R(5)	4709.8	P(4)
4626.6	R(6)	4722.3	P(5)
4519.6	R(7)	4730.1	P(6)
4662.9	R(8)	4736.6	P(7)

TABLE II
EXPERIMENTAL RESULTS

State	$\bar{k}_i \pm 2\sigma_{Mi}$, cc/sec/molecule x 10^9	$\bar{k}_i\tau_i$, cc/molecule x 10^{17}	$\sigma^2_{in}(i)$, $(Å)^2$	T, °K
n = 3	2.30 ± 0.14	2.3	76	290.6
4	0.97 ± 0.08	3.2	32	296.0
5	0.27 ± 0.02	2.3	8.9	291.4
$H_2G^1\Sigma_g^+$	0.94 ± 0.12*	0.94	38	292.2

*Assumed radiative lifetime of 10.0 nsec

UNCLASSIFIED

Security Classification

DOCUMENT CONTROL DATA - R & D

(Security classification of title, body of abstract and indexing annotation must be entered when the overall report is classified)

1 ORIGINATING ACTIVITY (Corporate author)

Arnold Engineering Development Center
Arnold Air Force Station, Tennessee 37389

2a. REPORT SECURITY CLASSIFICATION

UNCLASSIFIED

2b. GROUP

N/A

3 REPORT TITLE

COLLISIONAL DE-EXCITATION CROSS-SECTION MEASUREMENT OF ELECTRONIC STATES OF ATOMIC AND MOLECULAR HYDROGEN BY COLLISION WITH MOLECULAR HYDROGEN

4 DESCRIPTIVE NOTES (Type of report and inclusive dates)

Final Report - July 1, 1971 to March 1, 1972

5 AUTHOR(S) (First name, middle initial, last name)

J. W. L. Lewis and W. D. Williams, ARO, Inc.

6. REPORT DATE	7a. TOTAL NO. OF PAGES	7b. NO. OF REFS
October 1972	39	17

8a. CONTRACT OR GRANT NO.	9a. ORIGINATOR'S REPORT NUMBER(S)
b. PROJECT NO.	AEDC-TR-72-132
c. Program Element 65802F	9b. OTHER REPORT NO(S) (Any other numbers that may be assigned this report)
d.	ARO-VKF-TR-72-89

10 DISTRIBUTION STATEMENT

Approved for public release; distribution unlimited.

11 SUPPLEMENTARY NOTES	12. SPONSORING MILITARY ACTIVITY
Available in DDC	Arnold Engineering Development Center, Air Force Systems Command, Arnold AF Station, Tenn. 37389

13. ABSTRACT

The H_α, H_β, and H_γ lines of the Balmer series of atomic hydrogen and the $G^1\Sigma_g^+ \rightarrow B^1\Sigma_u^+$ molecular hydrogen system were produced by 40-kev electron beam excitation of molecular hydrogen at room temperature. The collisional de-excitation cross section of the above-mentioned excited electronic states in collision with H_2 $X^1\Sigma_g^+$ was measured.

DD FORM 1 NOV 65 1473

UNCLASSIFIED

Security Classification

14. KEY WORDS	LINK A		LINK B		LINK C	
	ROLE	WT	ROLE	WT	ROLE	WT
flow measurement						
hydrogen						
spectral lines						
electron beams						
fluorescence						
collision cross sections						

AFSC
Arnold AFS Tenn